ELSEVIER

Journal of Biomechanics 40 (2007) 1011–1023

JOURNAL OF BIOMECHANICS

www.elsevier.com/locate/jbiomech
www.JBiomech.com

Nanomechanical properties of individual chondrocytes and their developing growth factor-stimulated pericellular matrix

Laurel Ng[a,1], Han-Hwa Hung[b], Alexander Sprunt[c,2], Susan Chubinskaya[d], Christine Ortiz[e], Alan Grodzinsky[a,b,c,f,*]

[a]*Biological Engineering Division, Massachusetts Institute of Technology, 77 Massachusetts Avenue, Cambridge, MA 02139,USA*
[b]*Center for Biomedical Engineering, Massachusetts Institute of Technology, 77 Massachusetts Avenue, Cambridge, MA 02139, USA*
[c]*Department of Mechanical Engineering, Massachusetts Institute of Technology, 77 Massachusetts Avenue, Cambridge, MA 02139, USA*
[d]*Department of Biochemistry and Section of Rheumatology, Rush University Medical Center, Chicago, USA*
[e]*Department of Material Science and Engineering, Massachusetts Institute of Technology, 77 Massachusetts Avenue, Cambridge, MA 02139, USA*
[f]*Department of Electrical Engineering and Computer Science, Massachusetts Institute of Technology, 77 Massachusetts Avenue, Cambridge, MA 02139, USA*

Accepted 4 April 2006

Abstract

The nanomechanical properties of individual cartilage cells (chondrocytes) and their aggrecan and collagen-rich pericellular matrix (PCM) were measured via atomic force microscope nanoindentation using probe tips of two length scales (nanosized and micron-sized). The properties of cells freshly isolated from cartilage tissue (devoid of PCM) were compared to cells that were cultured for selected times (up to 28 days) in 3-D alginate gels which enabled PCM assembly and accumulation. Cells were immobilized and kept viable in pyramidal wells microfabricated into an array on silicon chips. Hertzian contact mechanics and finite element analyses were employed to estimate apparent moduli from the force versus depth curves. The effects of culture conditions on the resulting PCM properties were studied by comparing 10% fetal bovine serum to medium containing a combination of insulin growth factor-1 (IGF-1) + osteogenic protein-1 (OP-1). While both systems showed increases in stiffness with time in culture between days 7 and 28, the IGF-1 + OP-1 combination resulted in a higher stiffness for the cell-PCM composite by day 28 and a higher apparent modulus of the PCM which is compared to the FBS cultured cells. These studies give insight into the temporal evolution of the nanomechanical properties of the pericellar matrix relevant to the biomechanics and mechanobiology of tissue-engineered constructs for cartilage repair.

Keywords: Cartilage; Chondrocytes; Pericellular matrix; Nanomechanics; Nanoindentation; Growth factors

1. Introduction

Chondrocytes occupy only 3–5% of the volume of adult articular cartilage and, hence, do not contribute significantly to the bulk mechanical properties of the tissue (Stockwell and Meachim, 1979). However, they are responsible for the synthesis, maintenance, and turnover of the tissue's extracellular matrix (ECM). Mechanical loads and deformations applied to cartilage in vivo and in vitro are known to regulate chondrocyte synthesis and catabolic degradation of ECM macromolecules (Fitzgerald et al., 2004; Guilak et al., 1994; Kim et al., 1994; Valhmu et al., 1998). The mechanoregulation of chondrocyte metabolism in tissue engineering gel scaffolds depends partly on the cell's

*Corresponding author. Department of Electrical Engineering and Computer Science, Massachusetts Institute of Technology, 77 Massachusetts Avenue NE47-377, Cambridge, MA 02139, USA.
Tel.: +1 617 253 4969; fax: +1 617 258 5239.
E-mail address: alg@mit.edu (A. Grodzinsky).
[1]Currently at L-3 Communications/Jaycor, San Diego, CA, USA.
[2]Currently at ATA Engineering, San Diego, CA, USA.

0021-9290/$ - see front matter © 2006 Elsevier Ltd. All rights reserved.
doi:10.1016/j.jbiomech.2006.04.004

environment and the development stage of the newly synthesized, cell-associated pericellular matrix (PCM) (Buschmann et al., 1995).

The 2–4 μm thick PCM contains a high percentage of type VI collagen and proteoglycans (PGs) (Poole et al., 1992, 1988a) and is critically important to biochemical and biomechanical cellular function (Petit et al., 1996). The PCM transfers loads from the ECM to the cell and its cytoskeleton and intracellular organelles during physiologically induced deformations in compression, shear, and tension. The mechanical properties of individual chondrocytes with and without their PCM have been measured using micropipette aspiration (Guilak, 2000), cytoindentation (Koay et al., 2003), and in unconfined compression (Leipzig and Athanasiou, 2005). Apparent moduli of isolated chondrocytes (without PCM) were reported in the range 0.6–4 kPa from micropipette aspiration and compression of cells in agarose (Freeman et al., 1994). The PCM in adult cartilage has a higher modulus than the cell (~60–70 kPa) as measured via micropipette aspiration (Alexopoulos et al., 2003; Guilak et al., 1999), compression of chondrons in agarose (Knight et al., 2001), and AFM nanoindentation (Allen and Mao, 2004).

The PCM may also act as a regulator of cell signaling. Scaffolds seeded with chondrons containing intact PCM accumulated PGs and type II collagen more rapidly than parallel cultures of enzymatically isolated chondrocytes initially devoid of PCM (Graff et al., 2003). Chondrocytes treated with insulin-like growth factor (IGF-1) and osteogenic protein-1 (OP-1) showed increased PCM accumulation compared to chondrocytes maintained in fetal bovine serum (FBS) (Flechtenmacher et al., 1996; Loeser et al., 2003; McQuillan et al., 1986; Nishida et al., 2000; van Osch et al., 1998). Architecture and morphology of this newly developing PCM differ from adult chondron PCM. Adult chondron PCM appears as a compact structure in immunohistochemistry images of type VI collagen. PCM of immature tissue has more of a diffuse appearance (Lee and Loeser, 1998). Taken together, efforts to create tissue-engineered cartilage require detailed understanding of pericellular microenvironments.

In this study, we examined the mechanical properties of immature bovine cartilage chondrocytes and their newly developing PCM using atomic force microscope (AFM)-based indentation (i.e., measurement of force, F, versus indentation depth, D, on loading and unloading at two length scales via a nanosized tip (end-radius, R_{tip}~40 nm) and a micron-sized tip (R_{tip}~2.5 μm). The use of AFM to probe the mechanical properties of individual living cells has been reviewed (A-Hassan et al., 1998; Lehenkari et al., 2000a; Radmacher, 1997) and applied in the context of mechanotransduction (Charras and Horton, 2002), disease (Chasiotis et al., 2003), drug effects (Rotsch and Radmacher, 2000), and lysis kinetics (Hategan et al., 2003). To apply this technique to phenotypically round, nonadherent chondrocytes, we first developed microfabricated surfaces with wells to immobilize individual cells while keeping them viable. Freshly isolated chondrocytes, and cells released from 3D alginate gels after selected times in culture, were immobilized on these microfabricated surfaces, and studied nanomechanically to determine the effects of a newly developing PCM on cell-PCM stiffness. Cultures were supplemented with either FBS or the combination of IGF-1 + OP-1 to compare the effects of these anabolic stimulants on PCM development. The temporal evolution of cell-PCM biomechanical properties was compared to total GAG and collagen accumulation over time in culture by alginate-released cells. Apparent cell and PCM moduli were estimated from nanoindentation data using Hertzian contact mechanics and finite element analyses (FEA).

2. Materials and methods

2.1. Cell isolation and culture

Chondrocytes were isolated from femoral condyle cartilage of 2–3 week old bovine calves using sequential 0.2% pronase (Sigma) and 0.025% collagenase (Boehringer Mannheim) digestions previously (Ragan et al., 2000). Cell viability after isolation, assessed by trypan blue (Sigma) exclusion, was >95%. Cells were seeded at 20×10^6 cells/ml in 2% w/v alginate (KelcoLVCR) in 0.9% NaCl. Beads (~3 mm diameter) were formed through polymerization of droplets of alginate dispensed from a 22-gauge needle into 102 mM $CaCl_2$ solution. At selected times in culture, cells were released from alginate beads by depolymerization in a calcium chelator (Hauselmann et al., 1992; Petit et al., 1996), 55 mM NaCitrate, as described previously (Masuda et al., 2003). In one series of experiments, cell-seeded beads were maintained in hi-glucose Dulbecco's Modified Eagle Medium (DMEM) with 10% (v/v) FBS, 20 μg/ml L-ascorbic acid (Sigma), and 1% (v/v) antibiotic-antimycotic (Sigma). In a second series, cells were cultured in hi-glucose DMEM supplemented with 100 ng/ml recombinant human IGF-1 (PreproTech), 100 ng/ml recombinant human OP-1 (Stryker Biotech, Hopkinton, MA), mini-ITS (Benya and Padilla, 1993) (containing 5 nM insulin (Sigma) to minimize stimulation of the IGF-1 receptor, 2 μg/ml transferrin (Sigma), 2 ng/ml selenous acid (Sigma), 420/2.1 μg/ml linoleic acid-albumin from bovine serum albumin (Sigma)), 55 μg/ml L-ascorbic acid), and 1% (v/v) antibiotic-antimycotic. Seven alginate beads were cultured in 3 ml medium per well (12 well plate); medium was changed every other day.

2.2. Histology and immunohistochemistry of type VI collagen

Cells released from alginate were resuspended in culture medium (1×10^6 cells/ml) and fixed in 2% (v/v) glutaraldehyde solution (Polyscience) buffered with 0.05 M sodium cacodylate (Sigma), and containing 0.7% (w/v) of ruthenium hexaamine trichloride (RHT, Polyscience) to minimize loss of PGs during fixation (Hunziker et al., 1982). Fixed cells were mounted onto glass slides using a Cytospin (1400 rpm for 10 min), air dried, and stained for sulfated-PGs (Toluidine BlueO, Sigma) and collagen (phosphomolybdic acid followed by aniline blue (Rowley Biochemical)) (Luna, 1968). In addition, cells from day 39 culture were released, mounted on glass slides, dried for 3 h, treated with 2 mg/ml hyaluronidase (Sigma) in 0.1 M Tris(hydroxymethyl)aminomethane-HCl, pH 5.8, for 2.5 h at 37 °C to expose type VI collagen epitopes, then blocked with 5% donkey serum in PBS, pH 7.1, for 4 h. The antibody for type VI collagen (Chemicon) was incubated on the slides overnight (1:10 dilution in 1% donkey serum in PBS), then incubated with a secondary rhodamine-conjugated antibody (1:50 dilution in 1% donkey serum in PBS) for 4 h. Slides were rinsed with PBS after each step; fluorescently labeled cells were viewed using a Nikon TE300 microscope. Cell viability after release was >90% as assessed using fluorescein diacetate (0.2 mg/ml) and ethidium bromide (10 μg/ml) (Sigma).

2.3. Cell appearance and pericellular biochemical composition

Dimethyl methylene blue dye binding (DMMB) (Farndale et al., 1986) and hydroxyproline (Woessner, 1961) assays were used as measures of sulfated-GAG and collagen content, respectively. Optical micrographs of cells released at each time point were obtained to measure cell diameter and to aid in estimating PCM thickness.

2.4. Atomic force microscope imaging

Tapping mode AFM (TMAFM) images were taken of chondrocytes adsorbed on mica (SPI Supplies, West Chester, PA) in ambient conditions using a Multimode Nanoscope IIIa (Veeco, Santa Barbara, CA) and Olympus AC240TS-2 rectangular Si cantilevers ($k \sim 2$ N/m, $R_{tip} < 10$ nm).

2.5. Microfabrication of silicon substrates for single cell immobilization

Microfabricated substrates were prepared from silicon wafers at MIT's Microsystems Technology Laboratory and contained an array of inverted square pyramidal wells to hold a single cell in each well (Fig. 1a, b). Substrates with well side-dimensions of 15, 18, 20, or 22 μm were designed to hold freshly isolated cells and cells with associated PCM.

2.6. Nanoindentation

Silicon substrates were cleaned in piranha solution (3:1 (v/v) concentrated H_2SO_4/H_2O_2 (30%)) rinsed with acetone and DI water, and then immersed in DI water for 2 days. Culture medium was allowed to coat the silicon surface for 5 min. Then 100 μl of cell suspension was dropped onto the surface just prior to nanomechanical testing. The silicon wells, cells, and cantilever probe tip could be visualized with a $10\times$ optical microscope attached to the AFM (Fig. 1b). An AFM probe tip was used to push a cell laterally into a silicon well and then to perform nanoindentation loading–unloading cycles (Fig. 1c). The cell-containing well was identified and indentation was then repeated on the same cell using a second probe tip of different size (Fig. 1c). The Picoforce Nanoscope IV AFM (Veeco) was used to obtain indentation (F–D) data at z-piezo displacement rates of 200, 500 nm/s, 1, 3, 5 and 10 μm/s. No significant change in load–unload hysteresis was observed up to 1 μm/s. Above 1 μm/s, the area enclosed by the hysteresis loop increased in a logarithmic fashion. Therefore, to limit the contribution of cellular visco/poro-elastic effects to the measurements, data obtained at 1 μm/s are the focus of this paper (Supplementary Appendix A (Leipzig and Athanasiou, 2005; Koay et al., 2003; Collinsworth et al., 2002; A-Hassan et al., 1998)). A standard Si_3N_4 AFM square pyramidal tip (Veeco, $R_{tip} \sim 50$ nm, $k \sim 0.06$ N/m) and a colloidal probe tip were used. The colloidal probe tip was prepared using the AFM by attaching 2.5 μm radius silica beads (Bang Labs) onto tipless cantilevers (Veeco, $k \sim 0.06$ N/m) with low viscosity epoxy (SPI, MBond610). Cantilever spring constants were calibrated individually by the thermal oscillation method (Hutter and Bechhoefer, 1993).

2.7. Cell stiffness

Apparent elastic moduli were estimated from the nanoindentation data using 3 models: the Hertz model for a conical tip and a spherical (colloidal) tip, the slopes of stress/strain curves in the small strain region, and elastic FEA simulations. Analysis of cell moduli was limited to indentation depths less than 10% of the cell diameter, a small strain regime that minimized artifacts introduced from substrate effects (Tsui and Pharr, 1999).

FEA was carried out with ABAQUS (Providence, RI). One-fourth of the tip and cell were modeled; the well walls remained fixed in all directions, a frictionless boundary condition between the elastic cell and rigid

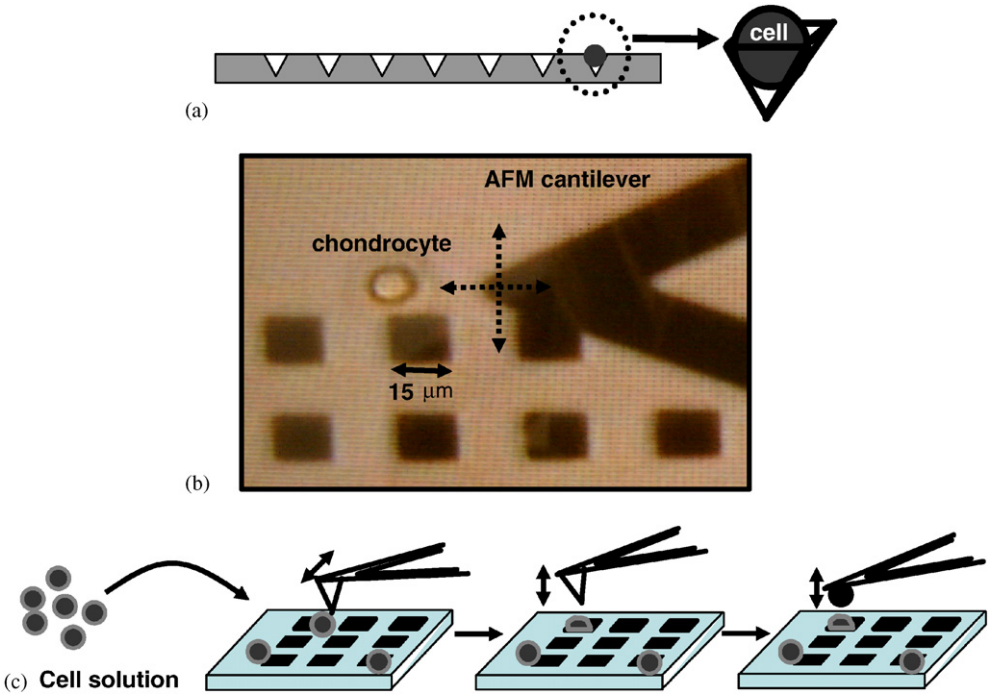

Fig. 1. (a) Schematic of micron-sized square pyramidal wells in a silicon substrate used for cell immobilization and nanomechanical measurements. (Indentation of chondrocytes was attempted on mica, but the flat surface was not suitable as the cells rolled away from the tip.) The wells were etched with a 20% (v/v) KOH solution using a silicon oxide hard mask of circles with diameters of 15, 18, 20, and 22 μm. The production of inverted square pyramids from circular mask openings is a consequence of anisotropy: (1 0 0) and (1 1 0) crystal planes are etched much more quickly than (1 1 1) planes, so self-terminating features bound by (1 1 1) planes are produced, forming planes 55° from the vertical (Kovacs et al., 1998). The masking oxide was thermally grown on 100 mm diameter single crystal silicon wafers and patterned with a Buffered Oxide Etch (BOE) using a photoresist mask. The photoresist was then stripped and the wafers placed in an 80 °C bath of 20% KOH for ~15 min until the etch self-terminated. The oxide mask was stripped with a second BOE and the wafer was singulated with a die-saw. The silicon surface was reusable after removal of organics with piranha solution (3:1 (v/v) concentrated H_2S0_4/H_2O_2 (30%)) followed by heat sterilization at 121 °C. (b) A 10 × optical microscope image of a single chondrocyte on a microfabricated silicon substrate and a 0.06 N/m Si_3N_4 cantilever used to maneuver an individual cell into a 15 μm inverted square pyramidal Si well. (c) After the cell was seated in a well, indentation was performed with the nanosized tip and then repeated on the exact same cell using the micron-sized tip.

well wall was used, and the displacement of the tip occurred only in the z-direction (normal to the cell) to ensure symmetry (see Supplementary Appendix B for details (Radmacher, 1997; Freeman et al., 1994; Petersen, 1982; Johnson and Greenwood, 1997; Jones et al., 1999; Leipzig and Athanasiou, 2005; Stolz et al., 2004; Lehenkari et al., 2000b; Freeman et al., 1994; Jones et al., 1999)).

2.8. Statistics

For PCM thickness and force–depth curves of individual cells ($n = 5$ replicate loading cycles applied to the cell), data are reported as mean ± SD. When averaging loading curves for multiple cells, with each cell subjected to five replicate loading cycles, data are reported as mean ± SE. Changes in PCM thickness were tested using ANOVA. The effects of depth and tip radius or culture time on indentation force were tested using two-way ANOVA. When significant effects ($p < 0.05$) were detected, comparisons between groups were performed using the Tukey post hoc test.

3. Results

3.1. Characterization of pericellular matrix

TMAFM images in ambient conditions show that freshly isolated cells (day 0) had no distinct PCM (Fig. 2a). After day 6 (10% FBS culture), a PCM layer was clearly observed (Fig. 2b is a typical image for day 11). By day 18 (Figs. 2c,d), type II collagen could be identified in the PCM as reported previously in alginate gel beads using immunohistochemistry and gel electrophoresis (Petit et al., 1996). Here, TMAFM showed fibril diameters of 59 ± 9 nm with a prominent small banding periodicity of 22 ± 2 nm, $n = 10$, likely associated with the 0.4D overlap zone within the primary $D = 67$ nm periodicity (Eyre, 2005; Hodge, 1967; Ortolani et al., 2000).

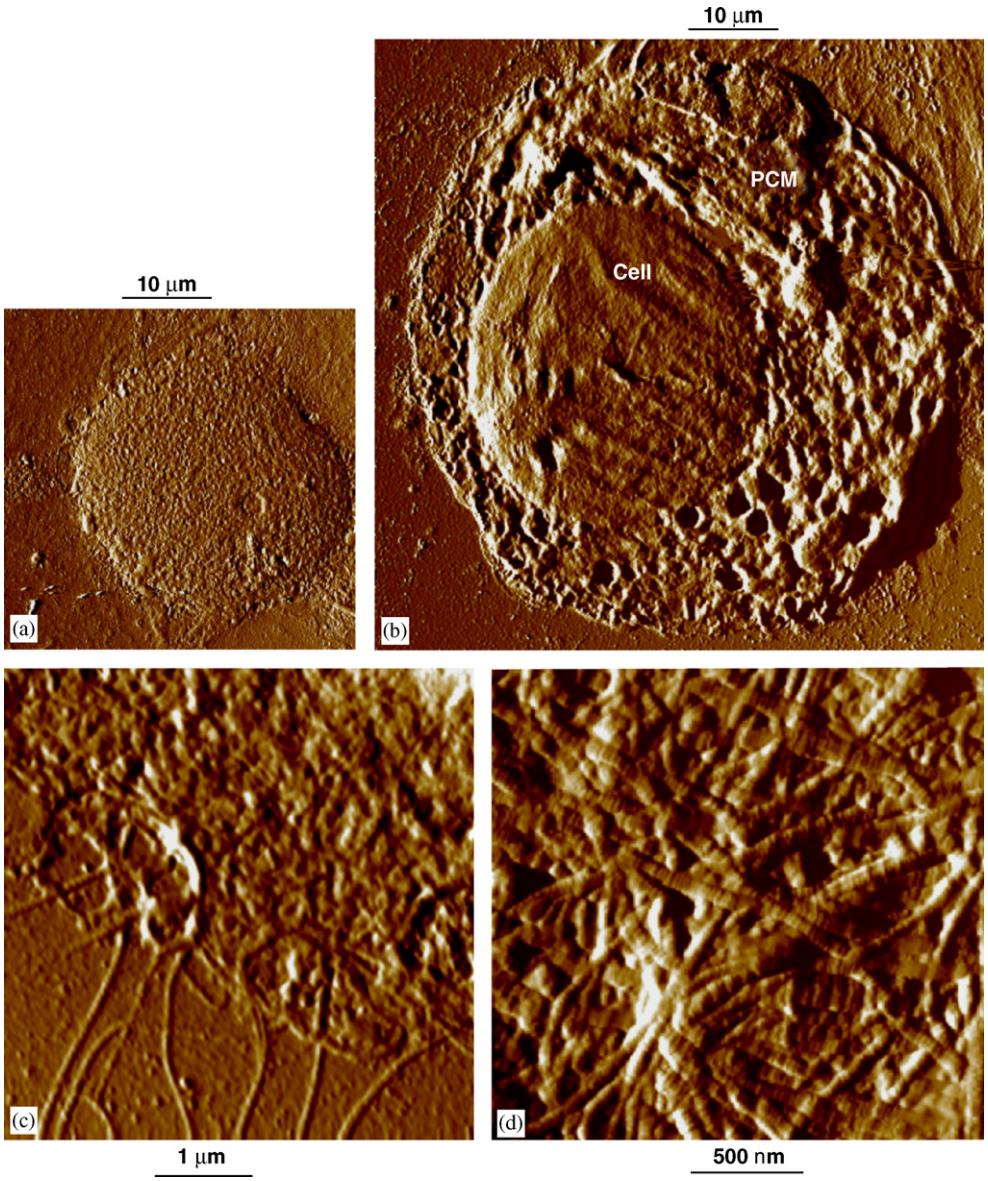

Fig. 2. Tapping mode amplitude AFM images in ambient conditions of calf chondrocytes adsorbed on mica substrates. (a) Freshly isolated chondrocyte (day 0), (b) chondrocyte released from alginate culture at day 11 where the PCM is clearly distinguishable from the cell body, (c) chondrocyte released from alginate culture at day 18 shows single collagen fibrils emanating out of the dense fibrillar network of the PCM, (d) a higher resolution image of the dense network which exhibit fibril diameter characteristic of type II collagen fibrils (Lodish et al., 2000). It should be noted that morphological features and cell surface roughness are likely altered by their sample preparation (for a review see (Shao et al., 1996)).

Optical microscopy images of fixed cells (Fig. 3) confirmed that freshly isolated cells (day 0) had no visible accumulation of PG or collagen. By day 7, PGs stained uniformly around the entire cell for both the FBS and IGF-1 + OP-1 cultures. Collagen staining was minimal for FBS, but distinct for IGF-1 + OP-1 cultures, both around the cell membrane and as a diffuse halo extending outward from the cell. By day 14, PG staining increased in diameter and intensity for both cultures, and collagen staining appeared around FBS cultured cells. By the third and fourth weeks in culture, no substantial changes in PG staining were observed, but collagen staining increased slightly in intensity and extent for both cultures. PG staining generally appeared greater with IGF-1 + OP-1 compared to FBS at all time points. While pericellular collagen staining appeared to extend further from the cell with IGF-1 + OP-1, staining intensity remained diffuse. Cell diameter (excluding PCM) was $7.65 \pm 0.85\,\mu m$ (mean $\pm$ SD). PCM thickness by optical microscopy was $\sim$3–4 μm between days 7 and 28, and did not change significantly during this time (Fig. 4a). Instances of dividing cells sharing matrix were observed, but were not used for nanoindentation. Cell viability in

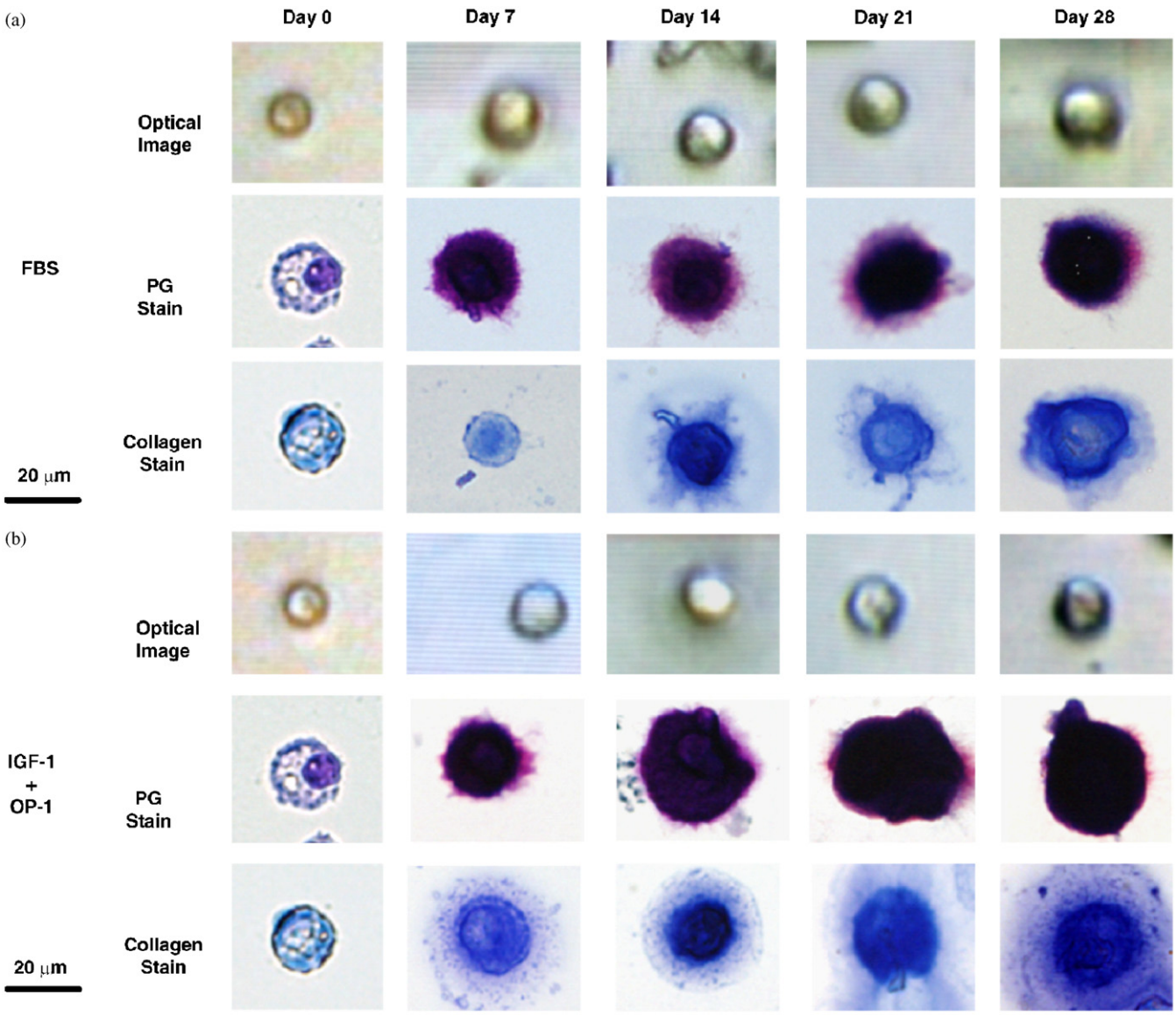

Fig. 3. Optical microscopy images (10 ×) of individual living calf chondrocytes and images (40 ×) of fixed calf chondrocytes released from alginate at different times in culture and stained for PG and collagen. (a) FBS supplemented medium and (b) IGF-1 + OP-1 supplemented medium. The top rows of (a) and (b) images were taken in culture medium. The middle rows show toluidine blue staining for PGs after day 7, which covered the entire cell surface, and extended over a larger diameter for cells cultured in IGF-1 + OP-1 compared to FBS supplemented medium. The bottom rows show aniline staining for collagen, which was generally not as uniform and intense as the PG stain.

gel culture remained above 80%, and chondrocytes retained their spherical phenotype (Fig. 3).

Type VI collagen was visible in the PCM of FBS (Fig. 4c) and IGF-1 + OP-1 cultured cells (not shown) processed at day 39, similar to that found in related experiments with same-aged bovine calf chondrocytes on days 7, 14 and 21 in agarose gel (DiMicco et al., 2005). Thus, these cells were capable of synthesizing and depositing this important component of the PCM in gel culture. Biochemical characterization showed that GAG and collagen content increased rapidly between days 0 and 14 in both cultures (Fig. 5). Between days 14 and 28, total collagen content did not appear to increase in either culture; GAG content continued to increase but was lower in FBS compared to IGF-1 + OP-1 cultured cells up to day 28.

3.2. Indentation of freshly isolated (day 0) cells

Indentation tests performed on single freshly isolated cells (day 0) using both the nanosized and micron-sized probe tips consisted of five sequential loading-unloading cycles averaged at one location at a displacement rate of 1 μm/s (Fig. 6). A nonlinear increase in repulsive force with indentation depth was observed; the small standard deviations for the five cycles indicated reversibility of

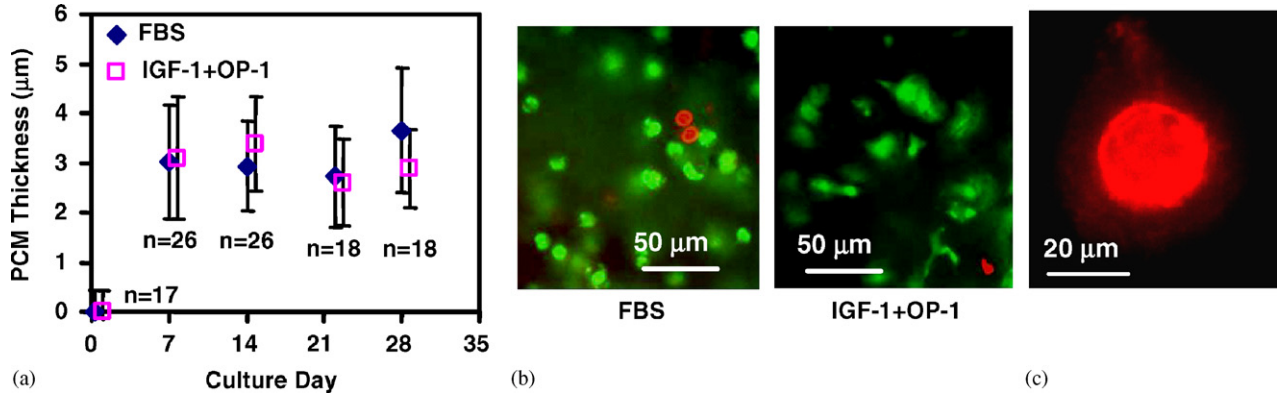

Fig. 4. Characterization of the PCM of living calf chondrocytes cultured in alginate using either FBS or IGF-1 + OP-1 supplemented medium. (a) An increase in PCM thickness (mean ± SD) measured from optical microscope images was observed from day 0 (freshly isolated cells) up to day 7; after day 7, PCM thickness did not change significantly (ANOVA, $p<0.05$; n = number of cells measured). PCM thickness was calculated as the average diameter measured at each time point minus the average diameter of freshly isolated cells (day 0) cells divided by 2. The error bars represent one standard deviation as calculated by a pooled sample variance. (b) Fluorescein diacetate and ethidium bromide showing live (green) and dead (red) cells on day 28 indicated >80% viability ($n = 20$). (c) Type VI collagen (immunohistochemistry) was present around both FBS (shown) and IGF-1 + OP-1 fed day 39 cells (not shown).

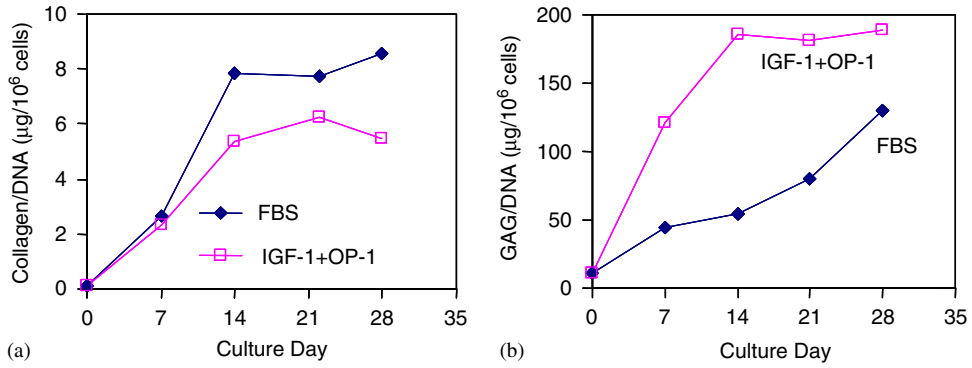

Fig. 5. Biochemical characterization of the PCM of calf chondrocytes released from alginate culture at designated time points corresponding to days that nanoindentation experiments were conducted. (a) Total GAG content of the PCM (measured by DMMB) was higher for cells supplemented with IGF-1 + OP-1 compared to FBS. (b) However, collagen content (measured by hydroxyproline) was similar for both cell cultures. Data were collected from 3 alginate beads pooled per condition per time point.

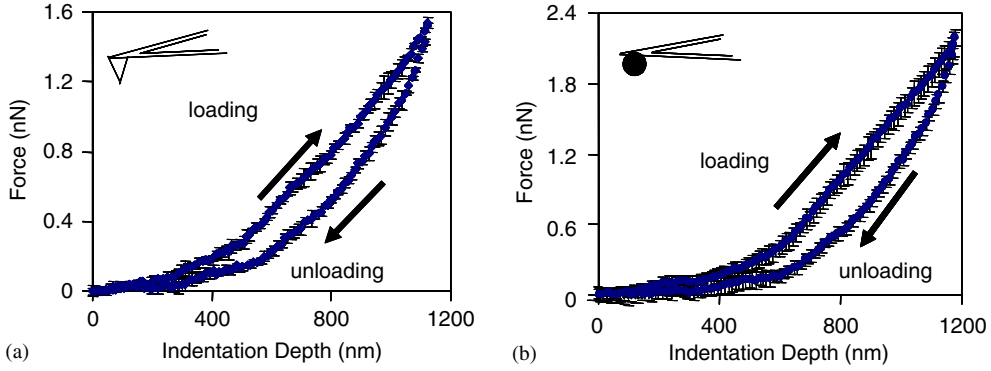

Fig. 6. Typical indentation curves of individual freshly isolated (day 0) calf chondrocytes. The tip–cell contact point was identified by a running average of the slope of every group of five data points until the calculated slope was greater than zero. Each plot shows 5 loading–unloading cycles (mean ± SD) for one cell immobilized in a silicon well using a z-piezo displacement rate of 1 μm/s with (a) a nanosized square pyramidal Si_3N_4 probe tip (R_{tip}~40 nm) and (b) a micron-sized colloidal probe tip (R_{tip}~2.5 μm).

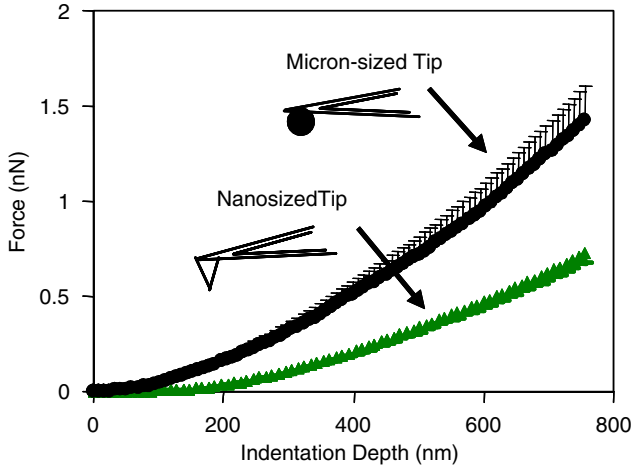

Fig. 7. Nanoindentation (on loading) of freshly isolated calf chondrocytes (day 0) using both the nanosized (mean ± SE for $n = 25$ cells with 5 loading cycles/cell, R_{tip}~40 nm) and micron-sized (mean ± SE for $n = 17$ cells with 5 loading cycles/cell, R_{tip}~2.5 μm) probe tips. (The same 17 cells were tested with both the nanosized and micron-sized probe tips.)

deformation after each cycle. Subsequent comparisons between days and culture conditions utilized only the nanoindentation data taken upon loading. For day 0 cells, the micron-sized probe tip produced significantly different forces than the nanosized probe tip at the same indentation depth ($p < 0.05$) (Fig. 7). The Hertz model predicted an apparent cell modulus between 0.7–1 kPa (Supplementary Appendix B). FEA simulations accounting for cell and tip geometry and boundary conditions (Fig. 8a) predicted an apparent cell modulus between 2.3–3 kPa for the micron-sized probe tip (Fig. 8b) (Supplementary Appendix B).

3.3. Indentation of cells with newly developing pericellular matrix

For cells in 10% FBS, both probe tips revealed stiffening of the cell-PCM composite with time in culture up to day 28 ($p < 0.05$) (Fig. 9a, b). For the nanosized probe tip, this stiffening with time was apparent for data in the range $D > 700$ nm, while for

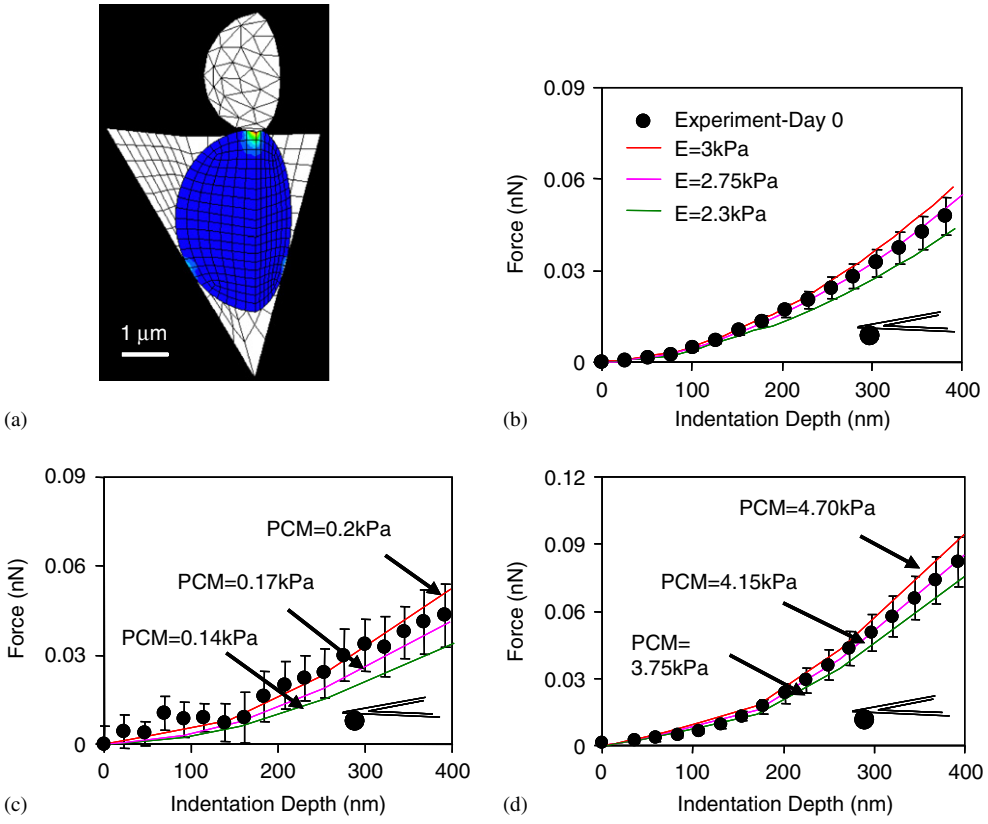

Fig. 8. (a) Elastic FEA model of nanoindentation experiment on chondrocytes with a micron-sized probe tip. (b) FEA model predictions using an apparent cell modulus of 2.75 kPa compared well to experimental data for indentation on loading of freshly isolated (day 0) cells ($n = 17$ cells, 5 loading cycles per cell) with micron-sized probe tip ($R_{tip} = 2.5$ μm). (c) Using a cell modulus of 2.75 kPa, shell thickness of 3.65 μm, cell radius $R_{cell} = 7.65$ μm, and Poisson's ratio = 0.4, the FEA shell model with a shell modulus of 0.17 kPa compared well with experimental data for day 28 FBS cultured cells ($n = 6$ cells, 5 loading cycles per cell). (d) Using a cell modulus of 2.75 kPa and a shell thickness of 3.65 μm, the FEA shell model with a shell modulus of 4.15 kPa compared well with the experimental data for day 28 IGF-1 + OP-1 cultured cells ($n = 5$ cells, 5 loading cycles per cell). Data are mean ± SE. Estimation of the cell modulus using FEA was limited to strains <10%. All analyses were done using a consistent indentation depth of 400. Based on the data, the modulus used in the FEA simulations was chosen to bracket the data of the force-indentation curves. See Supplementary Appendix B.4 for more details.

the micron-sized probe tip, stiffening was pronounced throughout most of the indentation range. Interestingly, the cell-PCM composites were always less stiff than the freshly isolated day 0 cells devoid of PCM ($p<0.05$) (Fig. 9a, b). For day 28 cells, the nanosized and micron-sized tips showed similar nanoindentation behavior for $D<900$ nm (Fig. 9c), while for $D>900$ nm, the nano-sized tip force exceeded the micron-sized tip at the same indentation depth.

Cell-PCM composites in IGF-1 + OP-1 also stiffened with time, observed with nanosized and micron-sized tips, and to a greater degree than the FBS cultured cells (Fig. 10). By day 28, cell-PCM composites were stiffer than freshly isolated day 0 cells ($p<0.05$) (Fig. 10). A modified FEA model of a cell with a surrounding elastic (PCM) shell, indented by the micron-sized tip, was used to estimate apparent moduli of the PCM. Using the apparent modulus of day 0 cells with no PCM (2.75 kPa, Fig. 8b) the shell modulus was varied until the model output matched the experimental data. For day21 FBS cultured cells, the shell modulus was 0.1 kPa and by day 28, the shell modulus increased slightly to 0.17 kPa. For the day 21 IGF-1 + OP-1 cultured cells, the shell modulus was 10 × stiffer than the FBS cultured cells at 1 kPa and by day 28, the shell modulus was 26 × stiffer at 4.15 kPa (Fig. 8d). See Supplementary Appendix B4 and Supplementary Table A1 for more details.

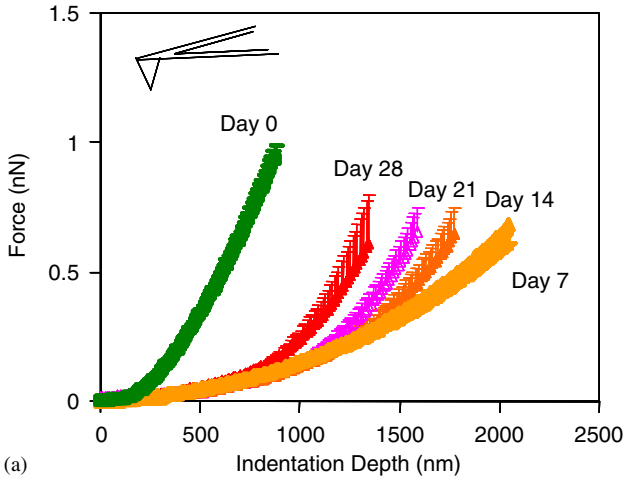

(a)

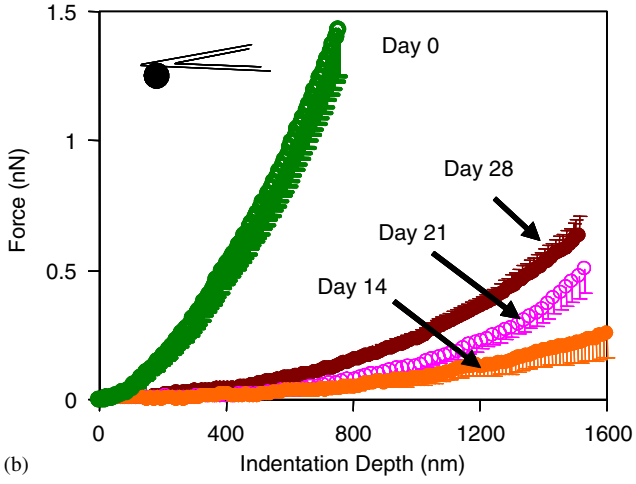

(b)

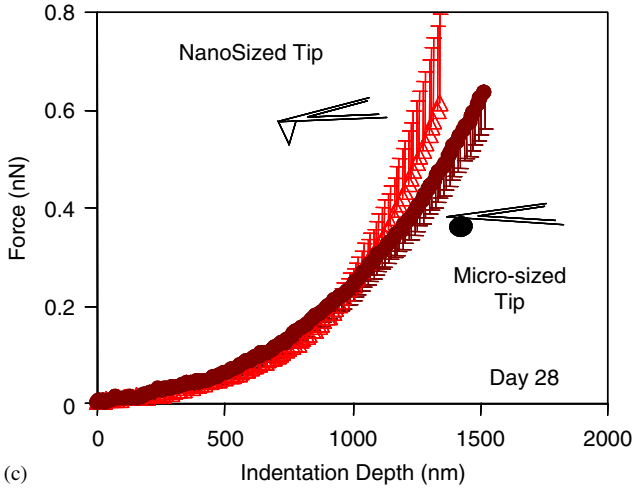

(c)

Fig. 9. Average indentation curves (mean ± SE of 5 loading cycles per cell on n cells) on loading of individual chondrocytes with their cell associated PCM after release from alginate at different times in culture with 10% FBS. (a) From the relative slopes of the F–D curves, the stiffness of the cell-PCM composite increased steadily from day 7 ($n=5$), to day 14 ($n=4$), 21 ($n=5$), and 28 ($n=6$), for the case of the nanosized probe tip (R_{tip}~40 nm). Even by day 28, however, the stiffness of the cell-PCM composite was lower than that of freshly isolated (day 0) cells devoid of PCM. (b) Similarly, F–D curves obtained with the micron-sized probe tip (R_{tip}~2.5 μm) showed stiffening of the cell-PCM composite with each week in culture, from day 14 ($n=4$) to day 21 ($n=5$) and 28 ($n=7$). (c) With day 28 cells, the F–D behavior with the micron-sized tip was similar to that of the nanosized tip for the first ~900 nm (nanosized probe tip: $n=6$; micron-sized probe tip: $n=7$).

4. Discussion

4.1. Mechanical properties of freshly isolated (day 0) cells

While the micron-sized probes interrogate cellular-scale properties, the small radius of curvature of nanosized probes are expected to be more sensitive to local cellular structures such as cytoskeletal elements and intracellular organelles. Nevertheless, the estimated modulus measured at both length scales was of the same order. This is in contrast to previously reported measurements on intact cartilage where the stiffness was 100 × greater with a micron-sized probe compared to a nanosized probe (Stolz et al., 2004). Hysteresis observed during the sequential, reversible loading/unloading cycles (Fig. 6) suggested the presence of

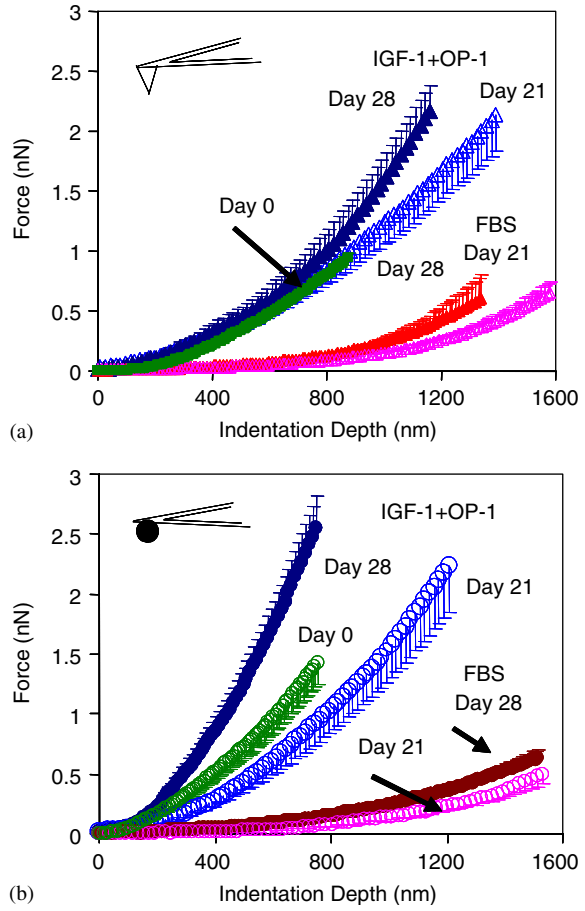

Fig. 10. Average indentation curves (mean ± SE of 5 loading cycles per cell for n cells per time point) on loading of individual calf chondrocytes with their PCM after released from alginate at different times in culture with IGF-1 + OP-1 supplemented medium. (a) Nanosized probe tip (R_{tip}~40 nm) data compared to 10% FBS data of Fig. 9a; the IGF-1 + OP-1 fed cells showed a marked increase in stiffness from days 21 to 28 ($n = 5$), and a higher force than cells in 10% FBS. (b) Micron-sized probe tip (R_{tip}~2.5 μm) data show an increase in stiffness from day 21 ($n = 5$) to day 28 ($n = 5$). In contrast to FBS cells of Fig. 9, day 28 IGF-1 + OP-1 cultured cells were stiffer than freshly isolated (day 0) cells as measured by the micron-sized probe tip, and for the nanosized tip (a) in the range $D > 700$ nm.

time-dependent material behavior (see Supplementary Appendix B.5 for estimates of viscoelastic properties (Cheng et al., 2005; Oyen and Cook, 2003; VanLandingham et al., 2005; Leipzig and Athanasiou, 2005; Shieh and Athanasiou, 2005; White et al., 2005; Mahaffy et al., 2004; Rico et al., 2005; Smith et al., 2005; Alcaraz et al., 2003; Leipzig and Athanasiou, 2005; Charras et al., 2005; Leipzig and Athanasiou, 2005)).

4.2. Pericellular matrix development

Developing PCM was confirmed and characterized using AFM imaging, measurement of collagen and GAG content, histological assessment of collagen and sulfated PGs, and immunofluorescence labeling of type VI collagen. The appearance of the PCM structure (e.g. a dense network of collagen fibrils) observed by TMAFM imaging (Fig. 2c,d) was similar to characteristic features of protease-digested native cartilage by TEM (Jurvelin et al., 1996) and AFM (Stolz et al., 2004). GAG and collagen accumulation with time in culture (Fig. 5) were qualitatively similar to that previously reported (Ragan et al., 2000), and the enhanced accumulation of GAG resulting from IGF-1 + OP-1 compared to FBS treatment was consistent with previous studies (Loeser et al., 2003). Histology showed a larger collagen-stained region for IGF-1 + OP-1 compared to the FBS fed cells, though likely more diffuse and containing less total collagen at later times (Fig. 5b). Type VI collagen (Fig. 4c), characteristic of the PCM, appeared as a diffuse halo around cells as seen by Lee and Loeser (1998), compared to the compact and more uniform PCM of fully developed chondrons (Poole 1997).

4.3. Mechanical properties of cells with developing PCM

Cell cultures supplemented with FBS or IGF-1 + OP-1 produced cells with a developing PCM that increased in stiffness from day 7 until day 28 in culture (Fig. 9). While the estimated thickness of the PCM did not change significantly after day 7 (Fig. 4a), GAG and collagen levels increased substantially from days 7 to 14, suggesting an increase in PCM density consistent with increased PCM stiffness (Fig. 9). However, IGF-1 + OP-1 cultured cells showed increases in stiffness despite a leveling of PGs and collagen. One explanation may be that the PCM is undergoing molecular organization of the small PGs and collagen, as well as collagen crosslinking (Chang and Poole, 1997; Eyre et al., 1987; Poole et al., 1988b). In addition, OP-1 has been found to help chondrocytes retain their developing PCM after release from alginate (Nishida et al., 2000). While the developing PCM appears to accumulate quickly in culture, the molecular structure and collagen architecture within the PCM may not resemble that of fully developed adult chondrons.

For the FBS fed cells, it was notable that the stiffness of the cell-PCM composite even after day 28 in culture was markedly less than that of freshly isolated cells, consistent with formation of a soft PCM of GAG, collagen, and other matrix molecules loosely organized around the cell membrane. As seen previously by immunofluorescence to the keratin sulfate antibody 5D4 (Lee and Loeser, 1998), newly developing matrix has a diffuse appearance. Thus, the early time PCM structure, when probed via indentation, had an apparent modulus less than the cell itself. Contrary to the freshly isolated cells (Fig. 7), the same amount of force was generated with the micron-sized tip and the nanosized tip up to D~900 nm (Fig. 9c). One hypothesis is that the

sharp nano-tip penetrated the developing PCM layer and came into closer contact with the stiffer cell membrane, thus generating as much force as seen by the larger micron-sized tip, which may not have easily penetrated the PCM and thereby sensed bulk PCM properties.

In comparison, the IGF-1 + OP-1 cultured cell-PCM composites released on day 28 showed a significant increase in stiffness over day 0 cells with both the probe tips (Fig. 10). Because the FEA had difficulty converging at depths greater than 200 nm for the nanosized tip due to the sharpness of the tip, we focus on FEA analysis with the micron-sized tip. For the first 600 nm, the shell model predicted the experimental data well and gave a PCM modulus of 0.17 kPa for the day 28 FBS cells (Fig. 8c), a value much lower than freshly isolated cells. The shell model compared well to the full range of data for the IGF-1 + OP-1 supplemented cells (shown in Fig. 8d for first 600 nm) giving a PCM modulus of 4.15 kPa, higher than that of freshly isolated cells (2.75 kPa). By comparison, the moduli of newly developing PCM for both cell treatments was much lower than that reported for native adult chondron PCM (Allen and Mao, 2004; Guilak et al., 1999) possibly due to the more mature PCM structure in adult tissue.

IGF-1 alone has been shown to increase proteoglycan content in newly developing PCM (van Osch et al., 1998). OP-1 has also been shown to increase proteoglycan (Nishida et al., 2000) as well as collagen synthesis and accumulation in newly developing PCM (Flechtenmacher et al., 1996). The combination of IGF-1 + OP-1 has been shown to increase cell division as well as promote proteoglycan content in the newly developing PCM (Loeser et al., 2003). IGF-1 + OP-1 treatment may cause additional modifications in PCM ultrastructure, including changes in macromolecular packing density and organization as well as increased collagen cross-linking.

4.4. Concluding remarks

In conclusion, a microfabricated surface was created to immobilize individual chondrocytes and their newly developing PCM to maintain a spherical phenotype during indentation tests. Apparent cell and PCM moduli were estimated from nanoindentation data using Hertzian contact mechanics and FEA. Temporal evolution of the cell-PCM composite in response to IGF-1 + OP-1 and FBS supplements in cell cultures showed that the former led to a greater GAG accumulation as well as a significant increase in stiffness observed by nanoindentation measurements, indicating perhaps a more developed PCM ultrastructure. For both cell cultures, the developing PCM properties showed increasing stiffness over a culture period of one month. A longer term study may reveal the kinetics by which continued increases in PCM stiffness could lead to the properties of fully developed chondrons, such as those measured via micropipette aspiration (Guilak et al., 1999; Jones et al., 1999) and AFM (Allen and Mao, 2004).

Acknowledgements

This work was supported by NSF-NIRT 0403903, NIH Grant AR33236, and a Whitaker Foundation Fellowship (LN). The authors would also like to thank Dr. Eliot Frank for contributions to viscoelastic modeling, and to the MIT Institute for Soldier Nanotechnologies funded through the US Army Research Office for use of instrumentation.

Appendix A. Supplementary Materials

Supplementary data associated with this article can be found in the online version at doi:10.1016/j.jbiomech.2006.04.004.

References

A-Hassan, E., Heinz, W.F., Antonik, M.D., D'Costa, N.P., Nageswaran, S., Schoenenberger, C.-A., Hoh, J.H., 1998. Relative microelastic mapping of living cells by atomic force microscopy. Biophysical Journal 74, 1564–1578.

Alcaraz, J., Buscemi, L., Grabulosa, M., Trepat, X., Fabry, B., Farre, R., Navajas, D., 2003. Microrheology of human lung epithelial cells measured by atomic force microscopy. Biophysical Journal 84, 2071–2079.

Alexopoulos, L.G., Haider, M.A., Vail, T.P., Guilak, F., 2003. Alterations in the mechanical properties of the human chondrocyte pericellular matrix with osteoarthritis. Journal of Biomechanical Engineering 125, 323–333.

Allen, D.M., Mao, J.J., 2004. Heterogeneous nanostructural and nanoelastic properties of pericellular and interterritorial matrices of chondrocytes by atomic force microscopy. Journal of Structural Biology 145, 196–204.

Benya, P.D., Padilla, S.R., 1993. Dihydrocytochalasin B enhances transforming growth factor-beta-induced reexpression of the differentiated chondrocyte phenotype without stimulaiton of collagen synthesis. Experimental Cell Research 204, 268–277.

Buschmann, M., Gluzband, Y.A., Grodzinsky, A.J., Hunziker, E.B., 1995. Mechanical compression modulates matrix biosynthesis in chondrocyte/agarose culture. Journal of Cell Science 108, 1497–1508.

Chang, J., Poole, C.A., 1997. Confocal analysis of the molecular heterogeneity in the pericellular microenvironment produced by adult canine chondrocytes cultured in agarose gel. Histochemistry Journal 29, 515–528.

Charras, G.T., Horton, M.A., 2002. Single cell mechanotransduction and its modulation analyzed by atomic force microscope indentation. Biophysical Journal 82, 2970–2981.

Charras, G.T., Yarrow, J.C., Horton, M.A., Mahadevan, L., Mitchison, T.J., 2005. Non-equilibration of hydrostatic pressure in blebbing cells. Nature 435, 365–369.

Chasiotis, I., Fillmore, H.L., Gillies, G.T., 2003. Atomic force microscopy measurement of cytostructural elements involved in

the nanodynamics of tumour cell invasion. Nanotechnology 14, 557–561.

Cheng, L., Xia, X., Scriven, L.E., Gerberich, W.W., 2005. Spherical-tip indentation of viscoelastic material. Mechanics of Materials 37, 213–226.

Collinsworth, A.M., Zhang, S., Kraus, W.E., Truskey, G.A., 2002. Apparent elastic modulus and hysteresis of skeletal muscle cells throughout differentiation. American Journal of Physiology: Cellular Physics 283, 1219–1227.

Dimicco, M.A., Kisiday, J.D., Gong, H., Grodzinsky, A.J., 2005. Fibrillar structure of type VI collagen-rich pericellular matrix assembled by agarose-embedded chondrocytes. Transactions of the Orthopaedic Research Society 30, 258.

Eyre, D., 2005. Personal communication.

Eyre, D.R., Apon, S., Wu, J.-J., Ericsson, L.H., Walsh, K.A., 1987. Collagen type IX: evidence for covalent linkages to type II collagen in cartilage. Federation of European Biochemical Societies (FEBS) Letters 220, 337–341.

Farndale, R.W., Buttle, D.J., Barrett, A.J., 1986. Improved quantitation and discrimination of sulphated glycosaminoglycans by use of dimethylmethylene blue. Biochimica et Biophysica Acta 883, 173–177.

Fitzgerald, J.B., Jin, M., Dean, D., Wood, D.J., Zheng, M.H., Grodzinsky, A.J., 2004. Mechanical compression of cartilage explants induces multiple time-dependent gene expression patterns and involves intracellular calcium and cyclic AMP. Journal of Biological Chemistry 279, 19502–19511.

Flechtenmacher, J., Huch, K., Thonar, E.J.-M.A, Mollenhauer, J.A., Davies, S.R., Schmid, T.M., Puhl, W., Sampath, T.K., Aydelotte, M.B., Kuettner, K.E., 1996. Recombinant human osteogenic protein 1 is a potent stimulator of the synthesis of cartilage proteoglycans and collagens by human articular chondrocytes. Arthritis and Rheumatism 39, 1896–1904.

Freeman, P.M., Natarajan, R.N., Kimura, J.H., Andriacchi, T.P., 1994. Chondrocyte cells respond mechanically to compressive loads. Journal of Orthopaedic Research 12, 311–320.

Graff, R.D., Kelley, S.S., Lee, G.M., 2003. Role of pericellular matrix in development of a mechanically functional neocartilage. Biotechnology and Bioengineering 82, 457–464.

Guilak, F., 2000. The deformation behavior and viscoelastic properties of chondrocytes in articular cartilage. Biorheology 37, 27–44.

Guilak, F., Jones, W.R., Ting-Beall, H.P., Lee, G.M., 1999. The deformation behavior and mechanical properties of chondrocytes in articular cartilage. Osteoarthritis and Cartilage 7, 59–70.

Guilak, F., Meyer, B.C., Ratcliffe, A., Mow, V.C., 1994. The effects of matrix compression on proteoglycan metabolism in articular cartilage explants. Osteoarthritis and Cartilage 2, 91–101.

Hategan, A., Law, R., Kahn, S., Discher, D.E., 2003. Adhesively tensed cell membranes: lysis kinetics and atomic force microscopy probing. Biophysical Journal 85, 2746–2759.

Hauselmann, H.J., Aydelotte, M.B., Schumacher, B.L., Kuettner, K.E., Gitelis, S.H., Thonar, E.J.-M.A, 1992. Synthesis and turnover of proteglycans by human and bovine adult articular chondrocytes cultured in alginate beads. Matrix 12, 116–129.

Hodge, A.J., 1967. Structure at the electron microscope level. In: Ramachandran, G.N. (Ed.), Treatise on Collagen. Chemistry of Collagen. Academic Press, London, pp. 185–205.

Hunziker, E.B., Herrmann, W., Schenk, R.K., 1982. Improved cartilage fixation by ruthenium hexammine trichloride (RHT). A prerequisite for morphometry in growth cartilage. Journal of Ultrastructure Research 81, 1–12.

Hutter, J.L., Bechhoefer, J., 1993. Calibration of atomic-force microscope tips. Review of Scientific Instruments 64, 1868–1873.

Johnson, K.L., Greenwood, J.A., 1997. An adhesion map for the contact of elastic spheres. Journal of Colloid and Interface Science 192, 326–333.

Jones, W.R., Ting-Beall, H.P., Lee, G.M., Kelley, S.S., Hochmuth, R.M., Guilak, F., 1999. Alterations in the Young's modulus and volumetric properties of chondrocytes isolated from normal and osteoarthritic human cartilage. Journal of Biomechanics 32, 119–127.

Jurvelin, J.S., Muller, D.J., Wong, M., Studer, D., Engel, A., Hunziker, E.B., 1996. Surface and subsurface morphology of bovine humeral articular cartilage as assessed by atomic force and transmission electron microscopy. Journal of Structural Biology 117, 45–54.

Kim, Y.-J., Sah, R.L.Y., Grodzinsky, A.J., Plaas, A.H.K., Sandy, J.D., 1994. Mechanical regulation of cartilage biosynthetic behavior: physical stimuli. Archives of Biochemistry and Biophysics 311, 1–12.

Knight, M.M., Ross, J.M., Sherwin, A.F., Lee, D.A., Bader, D.L., Poole, C.A., 2001. Chondrocyte deformation within mechanically and enzymatically extracted chondrons compressed in agarose. Biochimica et Biophysica Acta 1526, 141–146.

Koay, E.J., Shieh, A.C., Athanasiou, K.A., 2003. Creep indentation of single cells. Journal of Biomechanical Engineering 125, 334–341.

Kovacs, G.T.A., Maluf, N.I., Petersen, K.E., 1998. Bulk micromachining of silicon. Proceedings of the IEEE 86, 1536–1551.

Lee, G.M., Loeser, R.F., 1998. Interactions of the chondrocyte with its pericellular matrix. Cells and Materials 8, 135–149.

Lehenkari, P.P., Charras, G.T., Nesbitt, S.A., Horton, M.A., 2000a. New technologies in scanning probe microscopy for studying molecular interactions in cells. Expert Reviews in Molecular Medicine, 1–19.

Lehenkari, P.P., Charras, G.T., Nykanen, A., Horton, M.A., 2000b. Adapting atomic force microscopy for cell biology. Ultramicroscopy 82, 289–295.

Leipzig, N.D., Athanasiou, K.A., 2005. Unconfined creep compression of chondrocytes. Journal of Biomechanics 38, 77–85.

Lodish, H., Berk, A., Zipursky, S.L., Matsudaira, P., Baltimore, D., Darnell, J., 2000. Molecular Cell Biology. W.H. Freeman and Company, New York (pp. 981–985).

Loeser, R.F., Pacione, C.A., Chubinskaya, S., 2003. The combination of insulin-like growth factor 1 and osteogenic protein 1 promotes increased survival of and matrix synthesis by normal and osteoarthritic human articular chondrocytes. Arthritis and Rheumatism 48, 2188–2196.

Luna, E.G., 1968. Manual of Histological Staining Methods. McGraw-Hill Publication, New York (p. 94).

Mahaffy, R.E., Park, S., Gerde, E., Käs, J., Shih, C.K., 2004. Quantitative analysis of the viscoelastic properties of thin regions of fibroblasts using atomic force microscopy. Biophysical Journal 86, 1777–1793.

Masuda, K., Sah, R.L., Hejna, M.J., Thonar, E.J.-M.A, 2003. A novel two-step method for the formation of tissue-engineered cartilage by mature bovine chondrocytes: the alginate recovered chondrocyte (ARC) method. Journal of Orthopaedic Research 21, 139–148.

McQuillan, D.J., Handley, C.J., Campbell, M.A., Bolis, S., Milway, V.E., Herington, A.C., 1986. Stimulation of proteoglycan biosynthesis by serum and insulin-like growth factor-I in cultured bovine articular cartilage. Biochemistry Journal 240, 423–430.

Nishida, Y., Knudson, C.B., Kuettner, K.E., Knudson, W., 2000. Osteogenic protein-1 promotes the synthesis and retention of extracellular matrix within bovine articular cartilage and chondrocyte cultures. Osteoarthritis and Cartilage 8, 127–136.

Ortolani, F., Giordano, M., Marchini, M., 2000. A model for type II collagen fibrils: distinctive D-band patterns in native and reconstituted fibrils compared with sequence data for helix and telopeptide domains. Biopolymers 54, 448–463.

Oyen, M.L., Cook, R.F., 2003. Load-displacement behavior during sharp indentation of viscous-elastic-plastic materials. Journal of Materials Research 18, 139–150.

Petersen, K.E., 1982. Silicon as a mechanical material. Proceedings of the IEEE 70, 420–457.

Petit, B., Masuda, K., D'Souza, A.L., Otten, L., Pietryla, D., Hartmann, D.J., Morris, N.P., Uebelhart, D., Schmid, T.M., Thonar, E.J.-M.A, 1996. Characterization of crosslinked collagens synthesized by mature articular chondrocytes cultured in alginate beads: comparison of two distinct matrix compartments. Experimental Cell Research 225, 151–161.

Poole, C.A., 1997. Articular cartilage chondrons: form, function and failure. Journal of Anatomy 191, 1–13.

Poole, C.A., Ayad, S., Gilbert, R.T., 1992. Chondrons from articular cartilage. V. Immunohistochemical evaluation of type VI collagen organisation in isolated chondrons by light, confocal and electron microscopy. Journal of Cell Science 103, 1101–1110.

Poole, C.A., Ayad, S., Schofield, J.R., 1988a. Chondrons from articular cartilage: (I). Immunolocalization of type VI collagen in the pericellular capsule of isolated canine tibial chondrons. Journal of Cell Science 90, 635–643.

Poole, C.A., Flint, M.H., Beaumont, B.W., 1988b. Chondrons extracted from canine tibial cartilage: preliminary report on their isolation and structure. Journal of Orthopaedic Research 6, 408–419.

Radmacher, M., 1997. Measuring the elastic properties of biological samples with the AFM. IEEE Engineering in Medicine and Biology Magazine 16, 47–57.

Ragan, P.M., Chin, V.I., Hung, H.H., Masuda, K., Thonar, E.J.-M.A, Arner, E.C., Grodzinsky, A.J., Sandy, J.D., 2000. Chondrocyte extracellular matrix synthesis and turnover are influenced by static compression in a new alginate disk culture system. Archives of Biochemistry and Biophysics 383, 256–264.

Rico, F., Roca-Cusachs, P., Gavara, N., Farre, R., Rotger, M., Navajas, D., 2005. Probing mechanical properties of living cells by atomic force microscopy with blunted pyramidal cantilever tips. Physical Review Letters E 72, Art. No. 021914.

Rotsch, C., Radmacher, M., 2000. Drug-induced changes of cytoskeletal structure and mechanics in fibroblasts: An atomic force microscopy study. Biophysical Journal 78, 520–535.

Shao, Z., Mou, J., Czajkowsky, D.M., Yang, J., Yuan, J.Y., 1996. Biological atomic force microscopy: what is achieved & what is needed. Advances in Physics 45, 1–86.

Shieh, A.C., Athanasiou, K.A., 2005. Biomechanics of single zonal chondrocytes. Journal of Biomechanics, in press, doi:10.1016/j.biomech.2005.05.002.

Smith, B.A., Tolloczko, B., Martin, J.G., Grütter, P., 2005. Probing the viscoelastic behavior of cultured airway smooth muscle cells with atomic force microscopy: stiffening induced by contractile agonist. Biophysical Journal 88, 2994–3007.

Stockwell, R.A., Meachim, G., 1979. The chondrocytes. In: Freeman, M.A.R. (Ed.), Adult Articular Cartilage. Pitman Medical Publishing Co Ltd, Kent, pp. 69–144.

Stolz, M., Raiteri, R., Daniels, A.U., Vanlandingham, M.R., Baschong, W., Aebi, U., 2004. Dynamic elastic modulus of porcine articular cartilage determined at two different levels of tissue organization by indentation-type atomic force microscopy. Biophysical Journal 86, 3269–3283.

Tsui, T.Y., Pharr, G.M., 1999. Substrate effects on nanoindentation mechanical property measurement of soft films on hard substrates. Journal of Material Research 14, 292–301.

Valhmu, W.B., Stazzone, E.J., Bachrach, N.M., Saed-Nejad, F., Fischer, S.G., Mow, V.C., Ratcliffe, A., 1998. Load-controlled compression of articular cartilage induces a transient stimulation of aggrecan gene expression. Archives of Biochemistry and Biophysics 353, 29–36.

van Osch, G.J., van den Berg, W.B., Hunziker, E.B., Hauselmann, H.J., 1998. Differential effects of IGF-1 and TGF beta-2 on the assembly of proteoglycans in pericellular and territorial matrix by cultured bovine articular chondrocytes. Osteoarthritis and Cartilage 6, 187–195.

Vanlandingham, M.R., Chang, N.K., Drzal, P.L., White, C.C., Chang, S.-H., 2005. Viscoelastic characterization of polymers using instrumented indentation. I. Quasi-static testing. Journal of Polymer Science Part B-Polymer Physics 43, 1794–1811.

White, C.C., Vanlandingham, M.R., Drzal, P.L., Chang, N.-K., Chang, S.-H., 2005. Viscoelastic characterization of polymers using instrumented indentation. II. Dynamic testing. Journal of Polymer Science Part B-Polymer Physics 43, 1812–1824.

Woessner Jr., J.F., 1961. The determination of hydroxyproline in tissue and protein samples containing small amounts of this imino acid. Archives of Biochemistry and Biophysics 93, 440–447.